

## Direct Force Measurements at the Smooth Gold/Mica Interface

Randolph F. Knarr and Roger A. Quon

Department of Chemical Engineering, University of Pennsylvania, 220 South 33rd Street,  
311A Towne Building, Philadelphia, Pennsylvania 19104-6393

T. Kyle Vanderlick\*

Department of Chemical Engineering, Princeton University, Princeton, New Jersey 08540

Received February 3, 1998. In Final Form: July 27, 1998

We have developed a technique for accessing a very smooth gold surface (4 Å root-mean-square roughness) with nominal area greater than 100  $\mu\text{m}^2$ . It is a simple, controlled, and chemically noninvasive procedure of separating the smooth gold/mica interface carried out in the surface forces apparatus. Taking advantage of cold welding between surfaces of thin gold films and using carefully chosen quantities of compression, we have been able to isolate a region of the smooth gold/mica interface from forces other than those of adhesion. This allows measurement of the pull-off force required to separate smooth gold from mica ( $F_p/R = 1800$  mN/m); this represents a significant end point to data of previous studies addressing the impact of roughness on adhesion. Roughening of the gold surface during the separation process acts to reduce the pull-off forces required on subsequent separations.

### Introduction

The popularity of gold surfaces within the colloid and surface science community can be attributed to its highly desirable chemical and physical properties. While gold is chemically inert to many environments (oxidizing, acidic, basic, organic, etc.), its reactivity to thiol-headgroup molecules makes it an ideal substrate for structured, well-ordered monomolecular films known as self-assembled monolayers (SAMs).<sup>1,2</sup> A variety of tail groups such as alkyls, many biomolecular groups, fluorescent groups, carboxylic acid groups, and many other substituted organic entities can be anchored to the surface in an organized fashion through the sulfur-gold bond allowing the "tuning" of the chemical and physical properties of the gold surface.<sup>3-7</sup>

Because of the wide research applications of this noblest of metals, there has been a considerable effort by many groups to characterize gold surface properties.<sup>8-19</sup> SAM

chemists are especially interested in the characteristics of the surface and how they affect their monolayer's structure and resulting chemical and physical behavior.<sup>20-23</sup>

One such characteristic of interest is the surface roughness (or smoothness) of gold. The height of a typical alkyl-thiol SAM (which, of course, is dependent upon chain length, tilt angle, etc.)<sup>3</sup> is around 25 Å. This is on the same order or shorter than the root-mean-square (rms) roughness of typical underlying gold surfaces.<sup>14,15,24</sup> A smoother gold surface would allow researchers to probe more directly the effects of the SAM endgroup chemistry, chain length, chain structure, and mixture composition on the resulting monolayer properties while minimizing the interference from substrate topography. Analysis based on a two-dimensional view of SAMs, as is typically employed,<sup>3,25</sup> would better match the experimental situation if the gold substrate were as smooth as possible. Availability of a smooth surface of gold would also allow for the direct measurement of the fundamental work of adhesion of gold separation from other surfaces as has been accomplished in the well-studied case of mica/mica contact.<sup>26-29</sup> In reality, however, surfaces of thin gold films are rough.

A very convenient and economical source of a gold surface is a thin metallic film that is readily attained by

\* To whom correspondence should be addressed.

- (1) Troughton, E. B.; Bain, C. D.; Whitesides, G. M.; Nuzzo, R. G.; Allara, D. L.; Porter, M. D. *Langmuir* **1988**, *4*, 365.
- (2) Allara, D. L. *Biosens. Bioelectron.* **1995**, *10*, 771.
- (3) Sennett, R. S.; Scott, G. D. *J. Opt. Soc. Am.* **1950**, *40*, 203.
- (4) Pashley, D. W. *Philos. Mag.* **1959**, *4*, 324.
- (5) Smith, T. J. *Colloid Interface Sci.* **1980**, *75*, 51.
- (6) Culbertson, R. J.; Feldman, L. C.; Silverman, P. J. *Phys. Rev. Lett.* **1981**, *47*, 657.
- (7) Nogués, J.; Costa, J. L.; Rao, K. V. *Phys. A* **1992**, *182*, 532.
- (8) Sennett, R. S.; Scott, G. D. *J. Opt. Soc. Am.* **1950**, *40*, 203.
- (9) Pashley, D. W. *Philos. Mag.* **1959**, *4*, 324.
- (10) Smith, T. J. *Colloid Interface Sci.* **1980**, *75*, 51.
- (11) Culbertson, R. J.; Feldman, L. C.; Silverman, P. J. *Phys. Rev. Lett.* **1981**, *47*, 657.
- (12) Krim, J. *Thin Solid Films* **1986**, *137*, 297.
- (13) Hallmark, V. M.; Chiang, S.; Rabolt, J. F.; Swalen, J. D.; Wilson, R. J. *Phys. Rev. Lett.* **1987**, *59*, 2879.
- (14) Chidsey, C. E. D.; Loiacono, D. N.; Sleator, T.; Nakahara, S. *Surf. Sci.* **1988**, *200*, 45.
- (15) Naoi, Y.; Fukui, M. *J. Phys. Soc. Jpn.* **1989**, *58*, 4511.
- (16) Holland-Moritz, E.; Gordon, J., II; Borges, G.; Sonnenfeld, R. *Langmuir* **1991**, *7*, 301.
- (17) Watanabe, M. O.; Kuroda, T.; Tanaka, K.; Sakai, A. *J. Vac. Sci. Technol. B* **1991**, *9*, 924.
- (18) Golan, Y.; Margulis, L.; Rubinstein, I. *Surf. Sci.* **1992**, *264*, 312.

- (19) Nogués, J.; Costa, J. L.; Rao, K. V. *Phys. A* **1992**, *182*, 532.
- (20) Strong, L.; Whitesides, G. M. *Langmuir* **1988**, *4*, 546.
- (21) Creager, S. E.; Hockett, L. A.; Rowe, G. K. *Langmuir* **1992**, *8*, 854.
- (22) Camillone, N., III; Chidsey, C. E. D.; Liu, B.; Giacinto, S. *J. Chem. Phys.* **1993**, *98*, 4234.
- (23) McDermott, C. A.; McDermott, M. T.; Green, J.-B.; Porter, M. D. *J. Phys. Chem.* **1995**, *99*, 13257.
- (24) Levins, J. M.; Vanderlick, T. K. *J. Phys. Chem.* **1995**, *99*, 5067.
- (25) Whitesides, G. M.; Ferguson, G. S. *Chemtracts: Org. Chem.* **1988**, *1*, 171.
- (26) Tabor, D.; Winterton, R. H. S. *Proc. R. Soc. A* **1969**, *312*, 435.
- (27) Pashley, R. M. *J. Colloid Interface Sci.* **1981**, *80*, 153.
- (28) Pashley, R. M. *Chem. Scripta* **1984**, *25*, 22.
- (29) Horn, R. G.; Israelachvili, J. N.; Pribac, F. *J. Colloid Interface Sci.* **1987**, *115*, 480.

a multitude of methods including electroplating, sputtering, and evaporation. Evaporated gold surfaces are typically polycrystalline and are thus not atomically smooth, and this affects adhesion<sup>30–32</sup> as well as other surface phenomena. For example, the adhesion between a gold surface and molecularly smooth mica decays dramatically with increasing roughness.<sup>24</sup> This trend is very clear over a range of nonzero roughness from 20 to 70 Å length scale, but the limit as roughness tends to zero has escaped the realm of experimentation. With the best current preparation techniques, gold rms roughness over large areas (>25 μm<sup>2</sup>) of about 12 Å rms is routinely attainable,<sup>14</sup> but smoother still is a sought-after goal.

Investigators have tried to minimize the surface roughness of gold with varying degrees of success. One approach is to evaporate a thin film onto a molecularly smooth substrate. Mica can be cleaved along one molecular plane over areas larger than square centimeters<sup>14,16,33–36</sup> and is commonly used for employing this strategy. Presumably in the initial stages of growth, the gold will lie as smooth as possible next to the mica surface. The first few monolayers grow as islands in an epitaxial manner on the mica surface.<sup>11,14,16,18,37</sup> As the crystallites coalesce, the ultimate top surface morphology is being defined. Making the film thin minimizes propagation of surface defects and merging grains into roughness as can occur under certain deposition conditions.<sup>8,14</sup> Mica has the additional advantages of being mechanically, thermally, and chemically inert to various deposition techniques and subsequent processing of the gold.<sup>38</sup>

Refinement of gold deposition onto mica involves optimizing the evaporation conditions. Some investigators use evaporation rate to reduce roughness.<sup>8</sup> Substrate temperature during evaporation is another important variable.<sup>8,14,18,19,34,36</sup> Metal film post-treatment is yet another strategy for enhancing smoothness.<sup>14,17,18,35</sup> Thermal and chemical pre-treatments of the mica can all have influences on the roughness of the final, top surface of the gold.<sup>33,39</sup> A very thin underlayer metal, different from gold, can also be used to affect surface topography.<sup>14,11,35,36,39–41</sup> The use of different substrate materials altogether (e.g., silicon, quartz, graphite) results in other morphological characteristics of the gold surface.<sup>11,12,14,18,17,41–43</sup>

A technique based upon a different strategy involves accessing the gold surface at the gold/mica interface, that is, the backside gold surface. The original method, the

so-called “template stripped gold” (TSG)<sup>44,45</sup> process, has as its basis a very novel idea, but the approach is complicated and can lend itself to multiple occurrences of adsorption by soluble contaminants from either the bonding agent or detachment solvents. The exposed surface of the gold film on mica is glued down to a rigid pulling device such as a silicon wafer or a glass slide with either an epoxy or a ceramic glue. The gold is mechanically separated from the mica with or without the aid of a penetrating solvent to access the backside, smooth gold. This procedure produces large areas (25 μm<sup>2</sup>) of the smoothest gold known to date (~3 Å mean roughness). The key feature that makes the process viable is to ensure that the glue/top-gold-surface interface is stronger than the underlying smooth gold/mica interface. In fact in the case of the ceramic glues, the use of an adhesion promoter (thin different metallic layer plus silicon dioxide film) is necessary to accomplish the glue’s required “grip” on the top gold surface. Alternatively, adhesive tape can be used to remove successive layers of the mica until the backside gold surface is exposed. This process involves a somewhat uncontrolled mechanical separation and still requires epoxy or ceramic glue to anchor and support the gold film.

In the present work we access the backside gold surface using a simple technique that is controlled and chemically noninvasive, provides much larger areas (>100 μm<sup>2</sup>) of the smoothest gold surface known (4 Å rms roughness,  $R_a = 3$  Å), and in addition allows us to obtain an adhesion measure of gold to mica approaching the limit of a perfectly smooth interface. This adhesion sets an upper bound on the range of pulling forces that can be probed in systems for which a gold/mica underlayer is a required or convenient substrate. It also adds the yet unattainable smooth interface value to how adhesion depends on roughness for a metal/mica system. In addition, after initial separation, subsequent contacts can be examined to probe the effects of the separation process. Our technique is based on the unique capabilities of the surface forces apparatus (SFA).

### Creating and Characterizing a Very Smooth Gold Surface

As part of our ongoing research efforts studying metal/metal interfaces, we have examined the interactions between two gold films. Our findings show that the self-adhesion, namely cold welding, of two rough gold surfaces (~20 Å rms) is greater than the adhesion of the smooth gold/mica interface.<sup>46,47</sup> We substitute this strong and reliable metallic bond for the glue in the more complicated TSG technique described previously. Two gold films of unequal thickness (~400 and ~150 Å, respectively) are thermally evaporated (2.5–3.0 Å/s, room temperature, and 10<sup>-6</sup> Torr) onto two separate, molecularly smooth sheets of thin mica (~3 μm). The backside of the thinner gold film will eventually become the smooth gold surface. In dry nitrogen or air, these two gold surfaces, one of which is mounted on a force measurement spring, are brought to within a few hundred angstroms of each other using the SFA. At this point the surfaces spontaneously jump into adhesive contact because the van der Waals attractive forces overcome the resisting spring force. Upon contact, the gold surfaces cold weld together. The standard crossed cylinder arrangement of the two gold surfaces in the SFA

(30) Greenwood, J. A.; Williamson, J. B. P. *Proc. R. Soc. London A* **1966**, *295*, 300.

(31) Fuller, K. N. G.; Tabor, D. *Proc. R. Soc. London A* **1975**, *345*, 327.

(32) Levins, J. M.; Vanderlick, T. K. *J. Colloid Interface Sci.* **1997**, *185*, 449.

(33) DeRose, J. A.; Thundat, T.; Nagahara, L. A.; Lindsay, S. M. *Surf. Sci.* **1991**, *256*, 102.

(34) Buchholz, S.; Fuchs, H.; Rabe, J. P. *J. Vac. Sci. Technol. B* **1991**, *9*, 857.

(35) Carmi, Y.; Dahm, A. J.; Eppell, S. J.; Jennings, W.; Marchant, R. E.; Michal, G. M. *J. Vac. Sci. Technol. B* **1992**, *10*, 2302.

(36) Tangyonyong, P.; Thomas, R. C.; Houston, J. E.; Michalske, T. A.; Crooks, R. M.; Howard, A. J. *J. Adhesion Sci. Technol.* **1994**, *8*, 897.

(37) Sasajima, Y.; Tsukida, T.; Ozawa, S.; Yamamoto, R. *Appl. Surf. Sci.* **1992**, *60/61*, 653.

(38) Mica technical data sheet: (a) S&J Trading, Inc. Glen Oak, NY; (b) Mica New York Corp., New York, New York.

(39) Senden, T. J.; Ducker, W. A. *Langmuir* **1992**, *8*, 733.

(40) Liang, N. T.; Sheen, J. L.; Wang, S.-Y. *Surf. Sci.* **1988**, *206*, L921.

(41) Mae, K.; Inoue, Y.; Kyuno, K.; Kaneko, T.; Yamamoto, R. *Appl. Surf. Sci.* **1992**, *60/61*, 667.

(42) Clemmer, C. R.; Beebe, T. P., Jr. *Scanning Microscopy* **1992**, *6*, 319.

(43) Hecht, D.; Stark, D. *Thin Solid Films* **1994**, *238*, 258.

(44) Hegner, M.; Wagner, P.; Semenza, G. *Surf. Sci.* **1993**, *291*, 39.

(45) Wagner, P.; Hegner, M.; Güntherodt, H.-J.; Semenza, G. *Langmuir* **1995**, *11*, 3867.

(46) Levins, J. M. Ph.D. Thesis, University of Pennsylvania, Philadelphia, PA, 1994.

(47) Knarr, R. F.; Levins, J. M.; Vanderlick, T. K. To be submitted for publication.

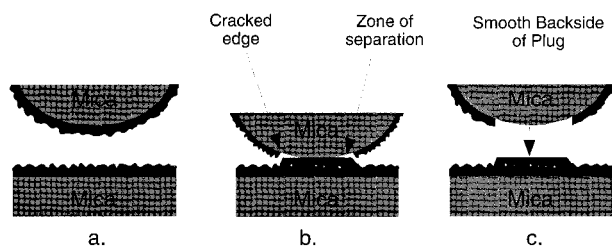


**Figure 1.** Plug-forming process carried out in the SFA: (a) two gold surfaces brought into adhesive contact cold weld together as soon as they touch, (b) compression and partial retraction has cracked the perimeter of the plug, the edges of which have begun the separation process, and (c) plug transferred to the opposing gold surface exposing the smooth backside of gold.

results in a small, but macroscopic, approximately circular area of contact (diameter  $\approx 40 \mu\text{m}$ ).

If the surfaces are then pulled and put into increasing tension, the gold surfaces do not separate, and the area of contact does not decrease, confirming that the two gold films are cold welded together. Instead, at some critical pulling force of about 35 mN, instantaneous failure occurs not at the newly formed gold/gold interface, but at one of the underlying smooth gold/mica interfaces. A plug of gold suddenly pops out of the thinner film and remains transferred to the thicker film (see Figure 1c). The now-exposed side of the plug, formerly the backside gold that was in contact with the opposing mica, is made accessible for further experimentation. However, this process involves shearing the perimeter of the contact zone of the thinner film as well as overcoming the gold/mica adhesion force in a single catastrophic event. While this method certainly provides access to the backside gold, it does not provide a gold/mica adhesion value. Furthermore, the plug size is limited to the contact area just before and during pulling as initially cold welded; we do note, however, that the area is larger than that obtained in the TSG process.

In the new technique we report here, we use the SFA to deliberately fracture the perimeter of the plug without the accompanying simultaneous, catastrophic separation. Once the perimeter of the contact zone in the thinner gold film is fractured (see Figure 1b), the shearing contribution to the resisting force is eliminated before the separation process is completed. This sequence isolates an intact, as-evaporated, smooth gold/mica interface for adhesion studies. To produce the broken perimeter, compression of the interface is required which necessarily and beneficially yields plugs of much larger area. Two related methods of fracturing the perimeter of the plug have evolved.

Instead of pulling after the initial jump into adhesive contact, if the surfaces are pushed together, the diameter of the contact region increases significantly and permanently via the cold welding process. In this first method, the compressive load is increased to about 55 mN force until a lateral displacement (on the order of  $1.5 \mu\text{m}$ ) of the surface is realized because of the arc-shaped path of the deflected leaf spring. The surface mounted on the end of the spring rolls relative to the opposing surface; this rolling behavior causes one side of the contact perimeter to suddenly crack. Using the optical capabilities of the SFA, we see distinct discontinuities in the interference fringes showing the crack at the edge of the contact zone very clearly. During subsequent pull back, as the surface "unrolls," the other side of the perimeter is cracked, again shown by the fringes. Rolling and unrolling are both required to completely fracture the entire perimeter as

shown in Figure 1b. Further retraction, but still with an overall net compressive force, yields an isolated gold/mica interface surrounded by a small finite ring of separation zone which in turn is surrounded by the cracked perimeter. We refer to this method as the rolling method.

The second method that we call the retraction method is similar to the first in that the surfaces are again pushed together, and the diameter of the contact region increases significantly and permanently because of cold welding. In this case, however, the surfaces are not compressed to the point of significant rolling. After sufficient compression to between 20 and 40 mN, the surfaces are then retracted back to the point of approximately zero average load. No change in contact area (i.e., the future plug area) is observed during this retraction. At a point in the return to zero load the perimeter of the contact zone will reach sufficient tension to crack the edge of the thinner gold film; the center of the region however remains in compression and adhered in a smooth gold/mica arrangement (see Figure 1b). Again the contact zone is surrounded by a ring of already-separated area within the cracked plug.

The use of compression in both methods not only serves to crack the perimeter of the plug but also to increase the plug diameter by more than 3-fold over the initial contact value. Both methods result in a cracked perimeter surrounding a separation zone that, in turn, surrounds an intact contact zone. In essence, the necessary steps to isolate the smooth gold/mica interface have resulted in the beginning of the separation process (see Figure 1b). In the language of contact mechanics, the gold/mica system is at some point on the "unloading curve" (which relates the contact diameter to the applied load).

That the perimeter of the plug is completely cracked all around its length can be verified by rotation of a dove prism in the optical path to check for the corresponding, characteristic discontinuity in the interference fringes. This is the case for both the rolling and the retraction methods. The smooth gold/mica interface has been isolated from all shear-force resistance in the gold film and will now behave in an unimpeded fashion in which diameter of the contact zone decreases with applied pulling force until separation. The standard method for measuring adhesion using the SFA can now be employed.<sup>26-28</sup>

With large areas of the backside gold available, characterization and comparisons can now be made. The new top side of the plug region and the normally exposed, as-evaporated surface have markedly different character. The surfaces were characterized with a Digital Instruments nanoscope III in tapping mode with 125 nm silicon cantilever (type TESP-DI) using a tip with radius of 5–10 nm. Atomic force microscopy (AFM) images (see Figure 2) show clearly that the two areas are texturally distinct. The roughness is also clearly different. In the plug region, it measures  $4 \text{ \AA rms}$  ( $R_a = 3.1 \text{ \AA}$ ) while in the evaporated area it is  $\sim 19 \text{ \AA rms}$  ( $R_a = 15.2 \text{ \AA}$ ).

### Measuring the Adhesion Force of the Smooth Gold Surface to Mica

The contact mechanics theory of Johnson, Kendall, and Roberts (JKR)<sup>48</sup> or that of others<sup>49</sup> can be employed to predict the fundamental work of adhesion of two bodies in contact from the pull-off force ( $F_p$ ) and out-of-contact relative radius of curvature of the two bodies ( $R$ ). Both quantities are directly measurable using the SFA in

(48) Johnson, K. L.; Kendall, K.; Roberts, A. D. *Proc. R. Soc. London A* **1971**, *324*, 301.

(49) Derjaguin, B. B.; Muller, V. M.; Toporov, Yu, P. J. *J. Colloid Interface Sci.* **1975**, *53*, 314.

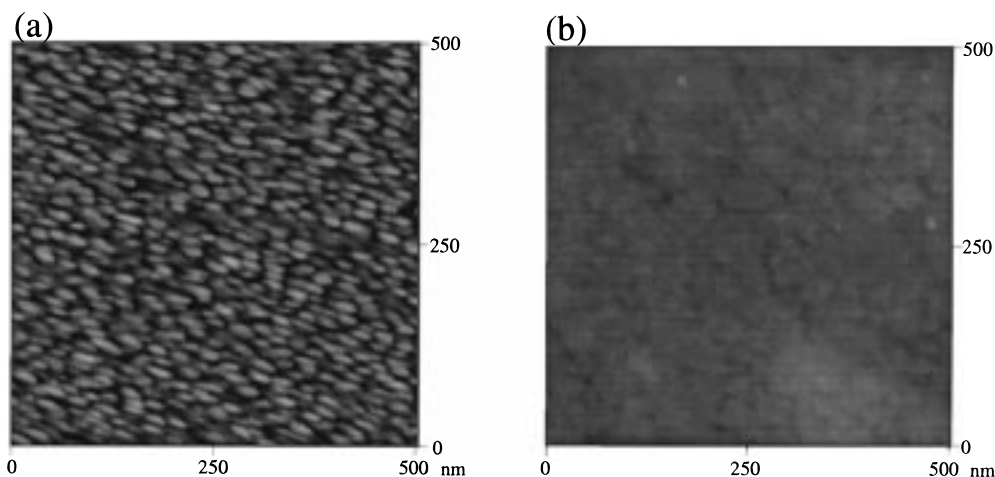


**Figure 2.** AFM image comparing the as-evaporated surface (a) with rms roughness of 18.7 Å ( $R_a = 15.2$  Å) to the newly exposed smooth gold surface and (b) with rms roughness of 4.0 Å ( $R_a = 3.1$  Å).

conjunction with multiple beam interferometry.  $F_p/R$  is proportional to the fundamental work of adhesion ( $F_p/R = -3/2\pi W$  in the JKR theory where  $W$  is the work of adhesion).

JKR theory also predicts how the relative geometry of two bodies in contact changes when they are subjected to an applied load. While the theory applies to both loading and unloading, we are restricted to unloading because of how we generate the smooth gold/mica interface. Again, the SFA in conjunction with multiple-beam interferometry can be used to measure the relevant quantities of contact diameter ( $D$ ) as a function of applied load ( $F$ ) until separation (pull-off). The behavior of  $D$  versus  $F$  depends only on the work of adhesion and the effective elastic constant of the system; these can then be determined by a least-squares fit to the data. Comparison of this estimate of work of adhesion (i.e., as obtained from the behavior of the detachment mechanics) to that obtained from the single pull-off force measurement provides a check on the applicability of the chosen theory to the system of interest.

Direct pull-off force measurement is the means by which Levins et al. studied the effect of a metal's roughness on its adhesion to mica.<sup>24</sup> Because only the crowns of the metal asperities touch and adhere to the mica surface, the space between them is filled with trapped dielectric material (air or nitrogen). In their studies, the roughness is then modeled as an equivalent air gap between the metal and the mica that the investigators characterized optically using extended spectral analysis of multiple beam interferometry<sup>50</sup> as applied in the SFA. For as-evaporated gold surfaces in contact with mica, this measure of roughness is 60 Å equivalent air gap with random error of up to 5 Å.<sup>24,32,51</sup> Using AFM we determined the step height of the plug to be 210 Å. This height represents the deposition thickness of gold (150 Å by quartz crystal microbalance in situ during evaporation) plus the thickness of the gold/gold cold-welded interface. Hence roughness modeled as equivalent air gap is consistent with this elevated step height value.

In the current work, after the plugs are fractured from the gold film, contact diameter during pull-off and ultimate pull-off forces were monitored. From the pull-off force measurement ( $F_p/R \approx 1800$  mN/m), we find the work of adhesion of the smooth gold/mica interface to be about 380 mN/m. This value is consistent with the JKR fit of

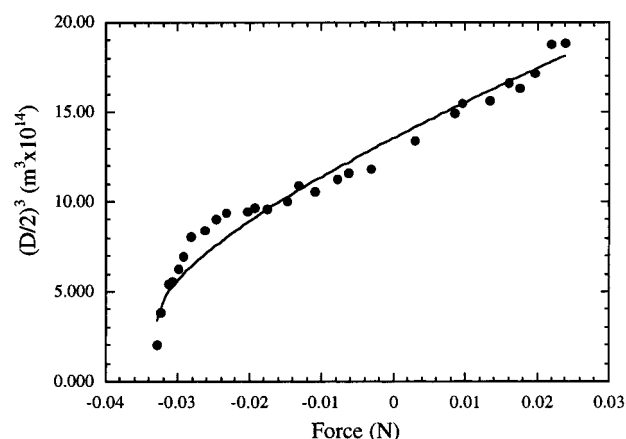


**Figure 3.** Behavior of contact diameter,  $D$ , (shown as  $[D/2]^3$ ) with applied load,  $F$ , during the initial unloading process after plug fracture. The solid curve is a least-squares fit of the JKR prediction with bulk elastic constant of the crossed cylinders ( $K = 1.96 \times 10^{10}$  N/m<sup>2</sup>) and fundamental work of adhesion of mica to gold ( $W = 0.344$  N/m) as fitting parameters.

the detachment mechanics obtained from unloading curves such as that shown in Figure 3. Measuring the adhesion of the smooth gold/mica interface represents a major step in completing the roughness/adhesion correlation ( $F_p/R$  vs roughness) begun by Levins et al.<sup>24</sup> As shown in Figure 4, addition of this new data point (corresponding to zero equivalent air gap) to those obtained previously shows that adhesion decays dramatically over the first few angstroms of roughness.

Previous studies have shown that prolonged contact between rough metal and mica causes the metal asperities to compress plastically, resulting in a smoother interface and increased adhesion with contact time.<sup>52</sup> Measuring the dynamics of the interface is accomplished by monitoring the equivalent air gap as a function of time. Externally applied loads affect the rate and extent of this smoothing process. Conversely, the separation process causes the gold surface to become rougher. This reroughening of the gold surface has been postulated to be caused by plastic, adhesive elongation of the contacting asperities.<sup>24,53</sup> As a result, when the surfaces are brought back into contact, the interface is rougher than before the previous separation.<sup>24</sup>

(50) Levins, J. M.; Vanderlick, T. K. *Langmuir* **1994**, *10*, 2389.

(51) Levins, J. M.; Vanderlick, T. K. *J. Colloid Interface Sci.* **1993**, *158*, 223.

(52) Levins, J. M.; Vanderlick, T. K. *J. Phys. Chem.* **1992**, *96*, 10405.

(53) Gane, N.; Pfaelzer, P. F.; Tabor, D. *Proc. R. Soc. London A* **1974**, *340*, 495.

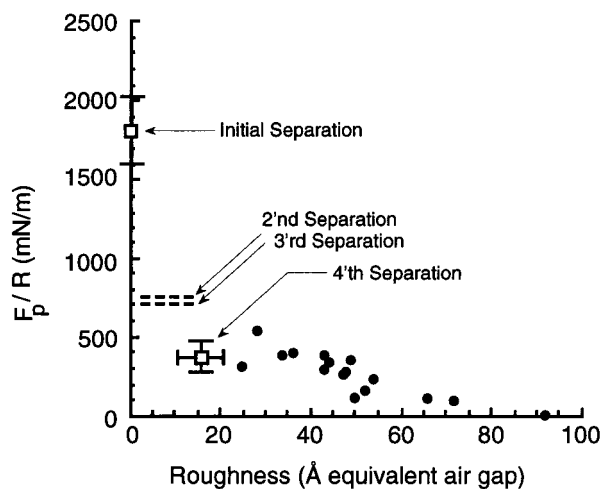


**Figure 4.** Adhesion (in terms of pull-off forces,  $F_p/R$ ) of metal to mica versus roughness of the interface. Roughness is given in terms of equivalent air gap as characterized using multiple beam interferometry. Most of the data is from Levins et al.<sup>24</sup> with two new data points from this work (for initial and fourth separations) as well as the levels of adhesion for intermediate reseparations (roughness not directly measured).

In our case, because the plugs are formed under compression, the area of zero-load recontact between the plug and opposing mica ( $D = 78 \mu\text{m}$ ) is smaller than the area of the plug itself ( $D_{\text{plug}} > 115 \mu\text{m}$ ), resulting in a recontact area well within the area of the plug. Therefore, making recontacts of the newly formed smooth gold surface with the opposing mica, that is, putting the plug back in the hole from which it came, without interference at the perimeter is not only possible, but quite easy. Being able to reinsert the plug in this way allows us to examine roughening caused by the separation process. The equivalent air gap measured upon the third reinsertion of the plug revealed a cumulative roughness increase of  $16 \text{ \AA}$ . Unfortunately, we neglected to make corresponding measurements after the first and second reinsertions; however, the AFM data taken on the exposed plug surface (obtained after the initial separation) shows a rms roughness of  $4 \text{ \AA}$ .

Subsequent recontacts after the initial, virgin separation yield progressively weaker adhesion, as shown in Table 1. The reduction is greatest from the first to the second separation and does not depend on whether the environment is dry nitrogen or dry air. These adhesion values can be added to the plot commenced by Levins et al.<sup>24</sup> showing pull-off force versus metal roughness, as illustrated in Figure 4. Our data points for the initial and fourth separation (i.e., after the third recontact) are shown; since equivalent air gap was not measured on the first and second recontact, dashed lines are used to signify the pull-off forces for these corresponding separations (note: as stated above, AFM measurements indicate a rms roughness of  $4 \text{ \AA}$ ).

Another contributing factor to the decrease in adhesion besides the roughening caused by the separation process is the possible adsorption of airborne contaminants to the

**Table 1.** Adhesion,  $F_p/R$  (mN/m), as a Function of the Number of Times the Surfaces Are Separated<sup>a</sup>

separation	$F_p/R$ (mN/m)		
	exp 1	exp 2	exp 3
1	1624	1851	1980
2	842	689	
3	781	634	
4	373		

<sup>a</sup> Adhesion values decrease as the number of recontacts increases. This could be caused by roughening of the gold surface and/or adsorption of contaminants over time. The first two recontacts were measured within 30 min of the original pull-off while the single third recontact was measured after the much longer time of 871 min.

gold, mica, or both. This trend over time was noted in mica/mica studies by Christenson who postulated that water is the contaminant in their case.<sup>54</sup> Trace carbonaceous and sulfurous contaminants could adsorb and interfere with subsequent contacts in our case, despite the steps taken to carefully eliminate them from the environment.<sup>10,12,14</sup> The initial smooth gold/mica interface was formed in a vacuum and is newly exposed to the dry nitrogen or air within the SFA during the first separation. Therefore, the first adhesion measurement is expected to be much less susceptible to such contaminants. Since we note no difference in the adhesion during recontacts in dry nitrogen and dry laboratory air, there is some evidence that contamination contributions are minor at worst over times of less than half an hour. However, over long times we have noted a more significant decrease in the adhesion after recontacts, as noted in Table 1.

### Summary

We have shown that very large areas ( $> 100 \mu\text{m}^2$  plugs) of the smoothest gold can be created using a controlled and chemically noninvasive technique in an inert atmosphere of dry nitrogen. The procedure is carried out in the surface forces apparatus taking advantage of cold welding phenomenon and using compression to isolate the smooth gold/mica interface for adhesion studies. Measurement of the adhesion of the smooth gold/mica interface ( $F_p/R = 1800 \text{ mN/m}$ ) adds the significant end point to how adhesion depends on roughness. Recontacts of the gold plug to mica results in reduced pull-off forces caused by adhesion-induced, plastic deformation of the surface creating or accentuating asperities and thus leading to roughness. Extension of this technique could be used to measure the adhesion of thin metal films to other materials of industrial interest such as polymers or ceramics.

**Acknowledgment.** We gratefully acknowledge support for this work from the National Science Foundation (CTS-9423780). We thank Bryan Huey of the University of Pennsylvania Laboratory for Research on the Structure of Matter SPM facility for helping with the AFM images.

LA980133M